

# Sequential Tunneling through Anisotropic Heisenberg Spin Rings

Jörg Lehmann and Daniel Loss

Department of Physics und Astronomy, Universität Basel,  
Klingelbergstrasse 82, CH-4056 Basel, Switzerland

(Dated: May 25, 2019)

We consider electrical transport through molecules with Heisenberg-coupled spins arranged in a ring structure in the presence of an easy-axis anisotropy. The molecules are coupled to two metallic leads and a gate. In the charged state of the ring, a Zener double-exchange mechanism links transport properties to the underlying spin structure. This leads to a remarkable contact-site dependence of the current, which for an antiferromagnetic coupling of the spins can lead to a total suppression of the zero-bias conductance when the molecule is contacted at adjacent sites.

PACS numbers: 85.65.+h, 85.75.-d, 75.10.Jm, 73.63.-b

*Introduction*—During the last decade, we have witnessed a tremendous progress in the experimental methods for contacting single molecules and measuring the electrical current through them [1–5]. A break-through has been achieved with the electromigration-junction technique [2], which allowed one to add a back-gate to the molecule, thereby bringing the whole field of Coulomb-blockade physics to molecular systems. Recently, this technique has led to the first transport measurements through single magnetic molecules: The current through the prototypical molecular magnet  $Mn_{12}O_{12}(\text{acetate})_{16}$  [6] has been measured and magnetic excited states have been identified [3, 4]. At the same time, various theoretical models for the description of these measurements have been put forward, all based on the effective Hamiltonians routinely used for the description of thermodynamic properties of the molecular magnet [3, 4, 7–9]. Doing so, an immediate complication encountered is that for the description of the sequential tunneling processes observed in the experiment, at least one charged state of the molecule has to be included in the model, as well. As plausible models for this state, the effective Hamiltonian with renormalized parameters [3, 7] or modified by a single additional orbital [8] have been employed.

In the present paper, we take a more microscopic approach based on a description of the constituent spins of the molecular magnet. Whereas this practically limits us to smaller systems than the ones considered experimentally, it enables us to readily include an excess charge. In particular, this will allow us to shed some light on the role of the orbital degree of freedom of this excess charge (say an electron) which cannot be treated using effective Hamiltonians only. Furthermore, we are able to consider on the same footing transport through antiferromagnetically coupled rings like molecular ferric wheels [10–14], which has not been studied so far.

Evidently, an excess electron will reduce one of the positively charged ions forming the localized spins. The arbitrary choice of this ion leads to an orbital degeneracy which will, however, be lifted by a hopping process between the different sites. At the same time, this hopping allows the electron to travel from one side of the molecule to the other and a current to flow across

the molecule. Since according to Hund’s rules, the coupling of the excess electron to the localized spin will favor one direction of the excess electron’s spin, and we assume that the hopping process leaves the spin of the electron unchanged [26], one obtains in the ground state an effective ferromagnetic type of coupling known as Zener double exchange [15–17]. Correspondingly, the orbital degree of freedom of the electron is interlinked with the spin structure of the ring and one should be able to observe this effect in the transport properties of the molecule. Here, the case of an antiferromagnetically coupled ring is of particular interest since double exchange is known to lead to a canting of the spin structure [17]. Due to the Néel ordered structure of the antiferromagnetic ground state, we even expect and confirm a strong even-odd-site-dependence of the current mediated by ground-state transitions, which are not present in the ferromagnetic case. Another intriguing property of antiferromagnetic rings is that quantum tunneling of magnetization (QTM) leads to a tunnel-split ground-state doublet with a characteristic oscillating dependence on the magnetic field [18]. We will demonstrate how this behavior can be extracted in a transport measurement.

*Model*—The physical picture described in the previous paragraph is captured by the Hamiltonian

$$H_0 = -J \sum_i \mathbf{S}_i \cdot \mathbf{S}_{i+1} - J_H \sum_i \mathbf{s}_i \cdot \mathbf{S}_i - k_z \sum_i (S_i^z + s_i^z)^2 + g\mu_B (\mathbf{S} + \mathbf{s}) \cdot \mathbf{B} - t \left( \sum_{i,\sigma} d_{i,\sigma}^\dagger d_{i+1,\sigma} + \text{h.c.} \right) + (\epsilon_0 - eV_g) n + Un(n-1)/2. \quad (1)$$

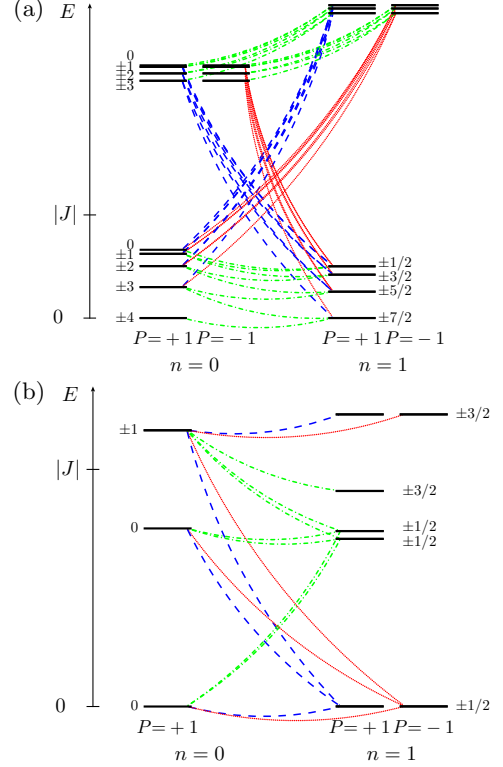
Here, the first term describes the Heisenberg coupling between the localized spins  $\mathbf{S}_i$  with spin quantum number  $s$ , where we require periodic boundary conditions  $\mathbf{S}_{N+1} = \mathbf{S}_1$  to describe a ring. The second term represents the Hund’s rule coupling of the excess spin when it is localized at the site  $i$  to the corresponding spin  $\mathbf{s}_i$ . The second-quantized spin operators  $\mathbf{s}_i$  are defined in terms of the creation (annihilation) operators  $d_{i,\sigma}^\dagger$  ( $d_{i,\sigma}$ ) for an electron of spin  $\sigma$  at site  $i$  by  $\mathbf{s}_i = (1/2) \sum_{\sigma\sigma'} \boldsymbol{\tau}_{\sigma\sigma'} d_{i,\sigma}^\dagger d_{i,\sigma'}$  with  $\boldsymbol{\tau}$  being the vector of

the three Pauli matrices. The spin of the excess electron is then given by  $\mathbf{s} = \sum_i \mathbf{s}_i$ . The easy-axis anisotropy of strength  $k_z$  and the Zeeman energy are included by the third and fourth term, respectively. The fifth term describes the hopping of the excess electron around the ring, where again periodic boundary conditions are assumed. The orbital energy  $\epsilon_0$  of the excess electron can be tuned by applying an external gate voltage  $V_g$  and is proportional to the occupation number  $n = \sum_i d_{i,\sigma}^\dagger d_{i,\sigma}$ . Finally, we restrict ourselves to a single excess electron by letting the charging energy  $U \rightarrow \infty$ .

The coupling of the molecule to the metallic leads is described by the tunnel Hamiltonian  $H_T = \sum_{\ell \mathbf{k} \sigma} T_{\ell \mathbf{k}} c_{\ell \mathbf{k} \sigma}^\dagger d_{i \sigma} + \text{h.c.}$  Here, the sum runs over the two leads  $\ell = L, R$ , which we assumed to be each coupled via a spin-independent coupling matrix elements  $T_{\ell \mathbf{k}}$  to a single ring site  $i_\ell$ . The leads at an electro-chemical potential  $\mu_\ell$  are modeled as a set of independent quasiparticles with wave-vector  $\mathbf{k}$  and spin  $\sigma$ ,  $H_L = \sum_{\ell \mathbf{k} \sigma} \epsilon_{\ell \mathbf{k}} c_{\ell \mathbf{k} \sigma}^\dagger c_{\ell \mathbf{k} \sigma}$ , distributed according to the Fermi distribution  $f(\epsilon - \mu_\ell) = \{1 + \exp[(\epsilon - \mu_\ell)/kT]\}^{-1}$ . Assuming that the externally applied bias voltage  $V_b$  drops completely and symmetrically along both molecule-lead contacts, we have  $\mu_{L,R} = \mu \pm eV_b/2$ , where  $\mu$  is the Fermi energy.

**Magnetic order**—The eigenstates  $|\alpha\rangle$  of the unperturbed ring Hamiltonian (1) can be separately considered for the cases of an uncharged ( $n = 0$ ) and charged ( $n = 1$ ) ring. Moreover, the discrete translational symmetry and the symmetry of reflection at an arbitrary site, say  $i = 1$ , yield corresponding good quantum numbers  $\cos(q)$  with  $-\pi < q \leq \pi$  and  $Nq = 0 \bmod 2\pi$ , and parity  $P = \pm 1$ , respectively. In the absence of a magnetic field with  $x$ - and  $y$ -components, another good quantum number  $M$  is given by the  $z$ -component of the total angular momentum  $\mathbf{S} + \mathbf{s}$ . For later use, we remark that the transition matrix elements  $\langle \alpha' | d_{i,\sigma}^\dagger | \alpha \rangle$  of the creation operator fulfil the selection rules  $n' - n = 1$  and  $M' - M = \sigma$ . Furthermore, in the special case  $N = 4$  considered below, we find  $P' = P$  for odd site numbers  $i = 1, 3$  and  $\exp(2iq)P' = \exp(2iq)P$  for even site numbers  $i = 2, 4$ .

We now discuss the magnetic order of the lowest-lying states for the two opposite cases of a ferro- and antiferromagnetic intra-ring coupling  $J$ . In both cases, we assume that the ions forming the localized spins have at least half-filled shells and thus consider according to Hund's rules a strong antiferromagnetic coupling  $J_H \ll -|J|$ . This describes, for instance, ferric wheels containing  $\text{Fe}^{3+}$  ions. We will exemplify the general discussion by the special case of a ring consisting of  $N = 4$  spins  $s = 1$  (cf. Fig. 1). The Heisenberg exchange coupling strength  $|J|$  serves as energy unit (typical values for ferric wheels range from 20 to  $30 k_B K$  [13]). The anisotropy is set to  $k_z = 0.3|J|$  and the Hund's rule coupling strength is  $J_H = -100|J|$ . An estimate for the hopping matrix element  $t$  is difficult to make. We assume  $t = 5|J|$ , which is consistent with the requirement that  $t/U' \approx J/4t \ll 1$ , where  $U'$  is the on-site charging energy and we have ap-



to the two lowest-lying quantum-mechanical eigenstates of the uncharged ring is then given by the symmetric and antisymmetric superposition of the two Néel states, i.e.,  $(|\uparrow\downarrow\rangle \pm |\downarrow\uparrow\rangle)/\sqrt{2}$ .

Similarly, in a purely classical picture and without hopping contribution, the *charged* ring has a  $2N$ -fold degenerate ground state which for an antiferromagnetic on-site coupling  $J_H < 0$  consists of the states  $|\uparrow\rangle|i,\uparrow\rangle$  and  $|\downarrow\rangle|i,\downarrow\rangle$  for odd  $i$  as well as  $|\uparrow\rangle|i,\downarrow\rangle$  and  $|\downarrow\rangle|i,\uparrow\rangle$  for even  $i$ . Here,  $|i,\sigma\rangle$  describes the state of the excess electron being localized at site  $i$  with spin  $\sigma$ . The hopping leads to an hybridization of the states of same Néel ordering and excess electron spin. Furthermore, QTM couples states with opposite Néel ordering of the localized spin lattice.

We find for the special case with  $N = 4$  and  $s = 1$  [cf. Fig. 1(b)] that the ground and first excited state of the uncharged ring are indeed dominated by the superposition of Néel-ordered states described above. The ground state of the charged ring turns out to be four-fold degenerate, discerning into two degenerate Kramers doublets with  $M = \pm 1/2$ . Focusing on the states with  $M = 1/2$ , we find that in the parity ( $P$ ) eigenbasis, the main contribution to the eigenstates stems from the states  $|\uparrow\rangle(|2,\uparrow\rangle - |4,\uparrow\rangle)$  with positive parity  $P = 1$  and  $|\downarrow\rangle(|1,\uparrow\rangle - |3,\uparrow\rangle)$  with negative parity  $P = -1$ . These states do not exhibit a QTM-induced tunnel splitting, which we attribute to a geometrical phase effect [19–21]. The situation is different for the two next excited Kramers doublets. The leading contribution to these states is given by the symmetric and antisymmetric combination of the two states  $|\uparrow\rangle(|1,\uparrow\rangle + |3,\uparrow\rangle)$  and  $|\downarrow\rangle(|2,\uparrow\rangle + |4,\uparrow\rangle)$  and we indeed observe a finite tunnel-splitting due to QTM.

*Master-equation approach*—We calculate the current through the ring using a Bloch-Redfield-equation approach to sequential tunneling, adapting and extending previous results of Refs. [22, 23]. In contrast to the standard Pauli master-equation description, this includes off-diagonal elements of the density-matrix to obtain a description also valid in the presence of (quasi-)degeneracies in the spectrum of the molecular Hamiltonian. It thus permits a description in the regime where the molecular levels are separated by less than  $\hbar\Gamma$ , where  $\Gamma$  is the typical tunneling rate from the molecule to the leads. We find that the dynamics of the density matrix elements  $\varrho_{\alpha\beta} = \text{Tr}_L \langle \alpha | \varrho | \beta \rangle$  after tracing out the leads is governed by the Bloch-Redfield equations

$$\dot{\varrho}_{\alpha\beta} = -i\omega_{\alpha\beta}\varrho_{\alpha\beta} + \frac{1}{2} \sum_{\ell\alpha'\beta'} \left\{ \left[ W_{\beta'\beta\alpha\alpha'}^\ell + (W_{\alpha'\alpha\beta\beta'}^\ell)^* \right] \varrho_{\alpha'\beta'} - W_{\alpha\beta'\beta'\alpha'}^\ell \varrho_{\alpha'\beta} - (W_{\beta\alpha'\alpha'\beta'}^\ell)^* \varrho_{\alpha\beta'} \right\}. \quad (2)$$

Here, we have introduced the frequencies  $\omega_{\alpha\beta} = (E_\alpha - E_\beta)/\hbar$  and the transition rates  $W_{\beta'\beta\alpha\alpha'}^\ell = W_{\beta'\beta\alpha\alpha'}^{\ell+} + W_{\beta'\beta\alpha\alpha'}^{\ell-}$  due to tunneling across a molecule-lead contact  $\ell$  in terms of the rates for tunneling of an electron on and off the molecule. These can be expressed as  $W_{\beta'\beta\alpha\alpha'}^{\ell+} = \sum_{\sigma i} \Gamma_\ell(E_\alpha - E_{\alpha'}) f(E_\alpha - E_{\alpha'} - \mu_\ell) \langle \beta' | d_{i_\ell,\sigma}^\dagger | \beta \rangle \langle \alpha | d_{i_\ell,\sigma} | \alpha' \rangle$

and  $W_{\beta'\beta\alpha\alpha'}^{\ell-} = \sum_{\sigma i} \Gamma_\ell(E_{\alpha'} - E_\alpha) [1 - f(E_{\alpha'} - E_\alpha - \mu_\ell)] \langle \beta' | d_{i_\ell,\sigma}^\dagger | \beta \rangle \langle \alpha | d_{i_\ell,\sigma} | \alpha' \rangle$ , respectively. Here,  $\Gamma_\ell(\epsilon) = (2\pi/\hbar) \sum_{\mathbf{k}} |T_{\ell\mathbf{k}}|^2 \delta(\epsilon - \epsilon_{\ell\mathbf{k}})$  is the spectral density of the coupling. Finally, the tunneling current across contact  $\ell$  can be determined from the density matrix elements via  $I_\ell = e \text{Re} \sum_{\alpha\alpha'\beta} (W_{\beta\alpha'\alpha'\alpha}^{\ell-} - W_{\beta\alpha'\alpha'\alpha}^{\ell+}) \varrho_{\alpha\beta}$ .

For the numerical solution of the master equation we cannot take all off-diagonal density-matrix elements, i.e., coherences, into account since the number of transition rates appearing on the right-hand-side of the master equation goes with the fourth power of the size of the system's Hilbert space. We thus only include coherences between energy eigenstates whose energies are not separated by more than the largest transition rate.

*Differential conductance*—For our numerical calculations, we use the model parameters described above. Additionally, the coupling to both leads is assumed to be contact- and energy-independent with a strength  $\hbar\Gamma = \hbar\Gamma_{\ell\sigma} = 0.01|J|$ . Figure 2 shows the differential conductance as a function of bias and gate voltage at zero magnetic field for both the ferro- and the antiferromagnetic case and for two different molecule-lead coupling variants: contacts at *opposite* and *adjacent*, respectively, sides of the ring. For a ferromagnetic coupling  $J > 0$ , the behavior in the low-bias-voltage regime is identical in both cases [see Figs. 2(a) and (b)]: the ground-state transitions dominate the current, and we are able to identify one excited state. A notable difference appears away from the charge-degeneracy point, where, for adjacent contacts, the  $n = 0 \rightarrow 1$  ground-state transition becomes suppressed. The mechanism behind this suppression is similar to the antiferromagnetic case [24], which will be discussed next.

In the case of an antiferromagnetic intra-ring coupling  $J < 0$ , we find a more striking difference between the two contacting situations. For adjacent contacts [see Fig. 2(d)], *the low-bias conductance is completely suppressed*, which does not occur for contacts at opposite sides [see Fig. 2(c)]. In order to understand this remarkable difference, we consider the magnetic order discussed above. There we identified two Kramers doublets of different parity in the  $n = 1$  ground state. Furthermore we found the selection rules depicted in Fig. 1 which depend on the site where the molecule is contacted. In particular, when contacting at adjacent sites, one contact only allows transitions to the even parity states and the other one only to the ones with odd parity. Thus, there is no transport path connecting both contacts and the current is blocked completely until transitions via excited states become possible at higher bias-voltages.

On the other hand, for contacts at opposite sides of the ring, only one parity state becomes populated and a current can flow. In this case, we observe a rather complex excited-state spectrum compared to the ferromagnetic case. For a better understanding of this regime, we focus on a fixed gate voltage as indicated by the arrow in Fig. 2(c) and consider in Fig. 3(a) the conductance as a function of an in-plane magnetic field [27].

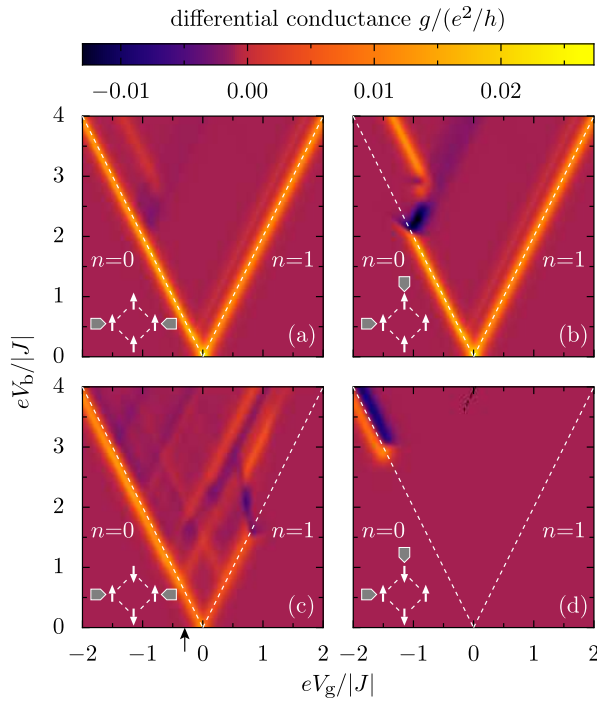


FIG. 2: (Color online) Differential conductance (color-coded) as a function of gate and bias voltage at zero magnetic field. The temperature is  $k_B T = 0.05|J|$  and the other parameters are as given in the main text. The upper two panels (a) and (b) show the conductance for a ferromagnetic coupling  $J < 0$ , the lower panels (c) and (d) depict the antiferromagnetic situation  $J > 0$ . The left (right) panels show the conductance when the molecule is contacted at opposite (adjacent) sites  $i_L = 1$  and  $i_R = 2$  ( $i_L = 1$  and  $i_R = 3$ ) (cf. inset schematic drawings). The dashed lines indicate the position of the ground-state transitions.

This dependence is particularly interesting for antiferromagnetic rings which, due to QTM, are very sensitive to such fields [18]. In particular, the tunnel splitting  $\Delta$  between ground and first excited state of the neutral ring [see Fig. 3(b)] oscillates as a function of the magnetic field. In order to extract this splitting from the conductance behavior, we identify all transitions between the lowest-lying states of the neutral and charged molecule (see labeled lines in Fig. 3). Denoting the magnetic-field dependent bias voltages at the corresponding resonances by  $V_{b,k}$  ( $k = 1, \dots, 4$ ), the tunnel splitting can be obtained as  $\Delta = e(V_{b,1} + V_{b,3})/2 = e(V_{b,2} + V_{b,4})/2$ .

We finally remark that a similar contact dependence of the current, albeit not a complete suppression of the

zero-bias conductance, has been predicted for benzene rings [25]. In this work, it was also noted that when excited states are populated, a non-tunneling decay may lead to a population of the odd-parity state such that for contacts on opposite sites one may find a current collapse at higher bias voltages. A similar scenario can be envisaged here with the additional possibility to lift the blockade again by applying a large-enough magnetic

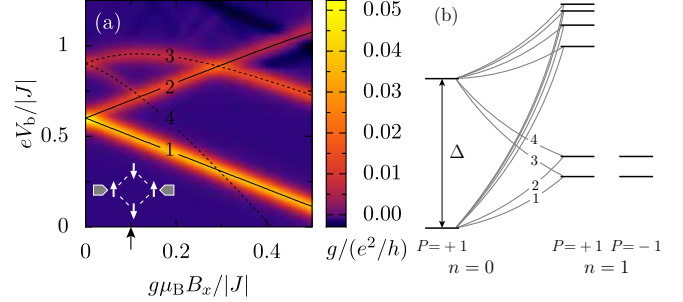


FIG. 3: (Color online) (a) Differential conductance through an antiferromagnetically coupled ring contacted at opposite sides as a function of magnetic field in  $x$ -direction and bias voltage. The gate voltage has been chosen as indicated by the arrow in Fig. 2(d). The temperature is  $k_B T = 0.01|J|$  and the other parameters are given in the main text. The solid (dashed) lines indicate the electron (hole) transition labeled in panel (b). (b) Level structure of ring and tunnel transitions for finite  $B_x$  as indicated by the arrow in panel (a).

field  $B_x$  [24]. Doing so, the current should display an interesting hysteretic behavior, which could possibly be employed for information storage purposes.

To conclude, we have presented a model for the description of a Heisenberg spin ring in the presence of a single excess electron. It contains a hopping term which both provides a transport path and results in a Zener double-exchange coupling between the localized spins. For an antiferromagnetically coupled ring, the interplay of these two effects leads to a strong contact-dependence of the sequential tunneling current through the molecule reflecting the Néel-ordered ground states. Our findings should not only be useful for the interpretation of transport experiments but also for the modelling of such systems when they are charged in an electro-chemical setup.

We thank D. Bulaev, B. Coish, J. Egues, and M. Wegewijs for discussions. Financial support by the EU RTN QuEMolNa, the EU NoE MAGMANet, the NCCR Nanoscience, and the Swiss NSF is acknowledged.

---

[1] *Molecular Electronics, Lecture Notes in Physics*, edited by G. Cuniberti, G. Fagas, and K. Richter (Springer, Berlin, 2005).  
[2] H. Park *et al.*, Appl. Phys. Lett. **75**, 301 (1999).  
[3] H. B. Heersche *et al.*, Phys. Rev. Lett. **96**, 206801 (2006).  
[4] M.-H. Jo *et al.*, arXiv:cond-mat/0603276 (2006).  
[5] C. F. Hirjibehedin, C. P. Lutz, and A. J. Heinrich, Science **312**, 1021 (2006).  
[6] R. Sessoli *et al.*, Nature (London) **365**, 141 (1993).  
[7] C. Romeike, M. R. Wegewijs, and H. Schoeller, Phys.

Rev. Lett. **96**, 196805 (2006).

[8] C. Timm and F. Elste, Phys. Rev. B **73**, 235304 (2006).

[9] M. N. Leuenberger and E. R. Mucciolo, arXiv:cond-mat/0604380 (2006).

[10] K. L. Taft *et al.*, J. Am. Chem. Soc. **116**, 823 (1994).

[11] A. Caneschi *et al.*, Chem. Eur. J. **2**, 1379 (1996).

[12] M. Affronte *et al.*, Phys. Rev. B **60**, 1161 (1999).

[13] B. Normand *et al.*, Phys. Rev. B **63**, 184409 (2001).

[14] A. Honecker *et al.*, Eur. Phys. J. B **27**, 487 (2002).

[15] C. Zener, Phys. Rev. **82**, 403 (1951).

[16] P. W. Anderson and H. Hasegawa, Phys. Rev. **100**, 675 (1955).

[17] P.-G. de Gennes, Phys. Rev. **118**, 141 (1960).

[18] A. Chiolero and D. Loss, Phys. Rev. Lett. **80**, 169 (1998).

[19] D. Loss, D. P. DiVincenzo, and G. Grinstein, Phys. Rev. Lett. **69**, 3232 (1992).

[20] J. von Delft and C. L. Henley, Phys. Rev. Lett. **69**, 3236 (1992).

[21] M. N. Leuenberger and D. Loss, Phys. Rev. B **63**, 054414 (2001).

[22] H.-A. Engel and D. Loss, Phys. Rev. Lett. **86**, 4648 (2001).

[23] S. Kohler, J. Lehmann, and P. Hänggi, Phys. Rep. **406**, 379 (2005).

[24] Details will be presented elsewhere.

[25] M. H. Hettler *et al.*, Phys. Rev. Lett. **90**, 076805 (2003).

[26] In principle, a spin flip during the hopping process can take place due to the on-site spin-orbit interaction which causes the anisotropy term. For simplicity, we disregard such an effect in the present model.

[27] Note that for the range of magnetic fields and bias voltages shown in Fig. 3(a), the current remains completely suppressed in the case of adjacent contacts (not shown).